High-resolution FTIR spectroscopy of CH2D35Cl: rovibrational analysis of the ν3, ν9 fundamentals and the 2ν6 - ν6, ν5 + ν6 - ν5 hot bands

Agostino Baldacci, Raffaella Visinoni, Santi Giorgianni, Giandomenico Nivellini

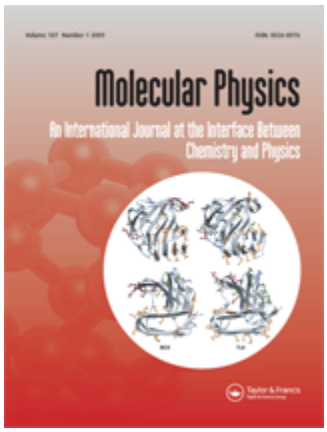

High-resolution FTIR spectroscopy of $CH_2D^{35}Cl$: rovibrational analysis of the ν_3, ν_9 fundamentals and the $2\nu_6 - \nu_6$, $\nu_5 + \nu_6 - \nu_5$ hot bands

Journal:	*Molecular Physics*
Manuscript ID:	TMPH-2008-0061.R1
Manuscript Type:	Full Paper
Date Submitted by the Author:	27-Mar-2008
Complete List of Authors:	BALDACCI, Agostino; Università Ca' Foscari di Venezia, Dipartimento di Chimica Fisica Visinoni, Raffaella; Università Ca' Foscari di Venezia, Dipartimento di Chimica Fisica GIORGIANNI, Santi; Università Ca' Foscari di Venezia, Dipartimento di Chimica Fisica Nivellini, GianDomenico; Università di Bologna, Dipartimento di Chimica Fisica e Inorganica
Keywords:	monodeutero methyl chloride, Fourier transform spectroscopy, vibration-rotation interaction

High-resolution FTIR spectroscopy of $CH_2D^{35}Cl$: rovibrational analysis of the ν_3, ν_9 fundamentals and the $2\nu_6 - \nu_6$, $\nu_5 + \nu_6 - \nu_5$ hot bands

A. Baldacci, R. Visinoni, S. Giorgianni

Università Ca′ Foscari di Venezia
Dipartimento di Chimica Fisica
D. D. 2137, I-30123 Venezia, Italy

and

G. Nivellini

Università di Bologna
Dipartimento di Chimica Fisica e Inorganica
Viale del Risorgimento 4, I-40136 Bologna, Italy

Running title: The ν_3, ν_9, $2\nu_6 - \nu_6$ and $\nu_5 + \nu_6 - \nu_5$ bands of $CH_2D^{35}Cl$

Corresponding author:

Prof. A. Baldacci

tel: +39-0412348508, fax: +39-0412348594

e-mail: baldacci@unive.it

No. of pages: 15
No. of figures: 6
No. of tables: 4

Abstract

The infrared spectrum of $CH_2D^{35}Cl$ has been measured on a Bomem Model DA3.002 Fourier transform spectrometer with a resolution of about 0.004 cm^{-1} and interpreted in the regions of the ν_9 (987 cm^{-1}) and ν_3 (1435 cm^{-1}) fundamentals. The unperturbed transitions of the weak ν_9 band have been analysed with the Hamiltonian of Watson to give accurate spectroscopic constants of the excited state. The transitions of the medium ν_3 band have been processed with a model which accounts for Coriolis and Fermi resonances with the $v_6 = 2$ state, located 16 cm^{-1} below the fundamental level. The rovibrational energy levels of this state, otherwise dark, have been obtained from the perturbation-allowed transitions observed in the ν_3 region and through a deeper analysis performed in the ν_6 spectral range, where a number of weak features have been assigned to the $2\nu_6-\nu_6$ and $\nu_5+\nu_6-\nu_5$ hot bands. Some spectroscopic parameters, in terms of an unperturbed level, have also been obtained for $v_5 = v_6 = 1$. Ground state constants have been improved using ground state combination differences (GSCDs) assembled from *a*-, *b*- and *c*-type transitions of four fundamentals. These new values allowed in turn the revision of the spectroscopic parameters of the coupled $v_5 = 1$ and $v_6 = 1$ states.

Deleted: Abstract

Deleted: medium

Deleted: of medium intensity,

Deleted: were

Deleted: are

Deleted: reported

1. Introduction

The halogenated methane derivatives are of interest as key chemical compounds. Among the monohalogenated series, the symmetric tops are currently studied through high resolution infrared spectroscopy by several laboratory groups in order to collect a data base that in the case of methyl chloride [1] and bromide [2] are useful for atmospheric applications. The less abundant methyl forms of the $^{35/37}$Cl isotopologues containing ^{13}C have also been object of investigation [3,4]. The methyl halides, with one or two substituted deuterium atoms, have received less attention since they are not included in the series of molecules considered as sources of anthropogenic nature. However, spectroscopic studies on these compounds are motivated by their importance for improving calculations of the general harmonic force field and ab initio potential energy surfaces [5].

Early studies performed on the series of partially deuterated methyl halides have been reported by Riter and Eggers [6]. The recent analysis on the monoisotopic $CH_2D^{35}Cl$ [7] provided the spectroscopic parameters obtained from the high resolution FTIR spectrum on the well separated fundamental bands ν_5 (827cm^{-1}) and ν_6 (714cm^{-1}). The results showed that the v_5=1 and v_6=1 states are mutually coupled through *c*-type Coriolis interaction and higher order anharmonic resonance. Ground state constants were determined for the first time pointing out that the low accuracy of the constants related to the principal moment of inertia was depending on the limited number of combination-differences with $\Delta K_a \neq 0$.

The present study has been undertaken to provide the spectroscopic parameters of the ν_9 and ν_3 bands of $CH_2D^{35}Cl$ centred at 987 cm^{-1} and 1435 cm^{-1}, respectively, and to optimize the ground state constants. The analysis was first devoted to the interpretation of ν_9 which shows the typical structure of an unperturbed *c*-type band. The derived GSCDs were merged with those obtained in [7] to improve the accuracy of the axial ground state constant values and adopted in the prediction of the line positions of the ν_3 band. The complex rotational structure of this fundamental of hybrid nature shows predominant *b*-type character compared to that of *a*-type. This band is perturbed by the $2\nu_6$ overtone expected to lie below of about 16 cm^{-1}. Additional perturbation effects observed at high K_a values can be attributed to the near higher state $v_5 = v_6 = 1$, at 1537 cm^{-1}, and to the lower states $v_8 = 1$ and $v_4 = 1$ at 1270 [8] and 1269 [6,7] cm^{-1}, respectively.

Deleted: Introduction

Deleted: (7

Deleted:)

Deleted: (6

Deleted:)

Deleted: and

Deleted: no

Deleted: in order

Deleted: two additional fundamental levels

Deleted: ground state combination-differences (

Deleted:), undergoing to the selection rules with ΔKa = ±1, ±2,

Deleted: 6

Deleted: globally

Deleted: are

Deleted: able

Deleted: other

Deleted: 11

In order to collect data on the most important perturber $2\nu_6$, we came back to the spectrum recorded in the ν_6 band region [7] and we assigned the weak structure of the $2\nu_6 - \nu_6$ and $\nu_5 + \nu_6 - \nu_5$ hot bands. This approach was based on the following statements: 1) the high purity sample of $CH_2D^{35}Cl$ avoided misassignment of lines due to the ^{37}Cl isotopologue, 2) the ν_6 fundamental, forming narrow clusters in the P and R branches, leaves large spectral sections free by strong absorptions, 3) the up to date ground state constants improved the ν_5=1 and ν_6=1 state parameters then employed for the lower states in the assignment of the hot bands.

After a brief description of the experiments, we discuss ~~on~~ the analysis of the ν_9, ν_3, $2\nu_6-\nu_6$ and $\nu_5+\nu_6-\nu_5$ bands. To follow, the refined spectroscopic constants of the ground and six vibrational states are given.

2. Experimental details

The monoisotopic sample of $CH_2D^{35}Cl$ was obtained in laboratory for spectroscopic purposes by reacting methyl-d1 alcohol with sodium chloride, containing 99% of ^{35}Cl, using the method previously described [7]. The separation of the product from the excess of the reagents was obtained by low temperature distillation under dynamic vacuum. The characterization of the sample, performed through standard IR techniques, showed the presence of HCl lines in the 2900 cm^{-1} region and of H_2O in the higher spectral range of the ν_3 band.

The high resolution (0.004 cm^{-1}, unapodized) spectrum was recorded at the University of Bologna using a Bomem Model DA3.002 Fourier transform spectrometer. The instrument was fitted with a conventional globar source, a potassium bromide beam splitter and a high sensitivity mercury-cadmium-tellurium (MCT) semiconductor as detector. Optical bandpass filters were employed in order to reduce the noise level of the spectrum. The covered region was between 850 and 1600 cm^{-1}, where four fundamentals are expected to produce absorption bands of different strengths. Hence the room temperature spectrum was recorded at the sample pressures of 40 and 173 Pa, using a multipass absorption cell with an optical path length of 5 m, by co-adding 713 scans. Calibration was done using the residual H_2O lines in the 1400-1600 cm^{-1} region, whose wavenumbers are mapped in [8]. The precision for unblended lines is about 0.0004 cm^{-1} and the accuracy is estimated to be better than 0.001

Deleted: 6
Deleted: the
Deleted: hot bands
Deleted: ¶ Experimental details
Deleted: preparation of the
Deleted: , CH_2DOH,
Deleted:
Deleted: NaCl,
Deleted: (6)
Deleted: 30
Deleted: 3.5μm region
Deleted: in the upper spectral range
Deleted: levels
Deleted: In total 713 scans were coadded for both recordings
Deleted: ref.

cm^{-1}. The measured full width at half maximum (FWHM) at 987 and 1435 cm^{-1} is 0.004 and 0.006 cm^{-1}, respectively. Details of the spectrum recorded in the ν_6 band region, obtained with the same FTIR spectrometer, are given in [7].

3. General remarks

The monodeutero methyl chloride is a near prolate asymmetric top ($\kappa = -0.978$) of point group C_s. The nine normal modes divide into two symmetry classes, A′ and A″, all active in the infrared. Six of them (ν_1 - ν_6) are expected to give rise to *a*/*b*-hybrid bands, where one of the components is often predominant, and three (ν_7 - ν_9) should manifest *c*-type envelopes. The ν_9 fundamental appears therefore of *c*-type, ν_3 is representative of a structure where the *b*-type component prevails, while $2\nu_6 - \nu_6$ and $\nu_5 + \nu_6 - \nu_5$, similarly to ν_6, show the typical structure of pure *a*-type bands. On the whole, the spectral characteristics approach those of parallel (*a*-type) and perpendicular (*b*- and *c*-type) bands of symmetric tops.

The rovibrational structure has been interpreted by adopting the Watson's A-reduction Hamiltonian in the I^r representation [10] adequately implemented with perturbation operators when the interactions were taken into account. The rovibrational assignment has been performed by applying the usual selection rules for *a*-, *b*- and *c*-type bands. In the present investigation the identified transitions undergo to:

a-type bands: $\Delta J = 0, \pm1, \Delta K_a = 0, \Delta K_c = \pm1$,

b-type bands: $\Delta J = 0, \pm1, \Delta K_a = \pm1, \Delta K_c = \pm1$,

c-type bands: $\Delta J = 0, \pm1, \Delta K_a = \pm1, \Delta K_c = 0, \pm2$.

The perturbation-allowed transitions, attributed to $2\nu_6$ and observed in the ν_3 band region, follow the selection rules:

$\Delta J = 0, \pm1, \Delta K_a = 0, +1, +2, \Delta K_c = \pm1, -3$

The assignment of ν_9 and ν_3 has been performed using an iterative process based on the identification of new transitions and improvement of the ground and upper state constants, while that of the hot bands has been ~~provided on~~ assisted by the lower state combination differences obtained from the refined constants of the $\nu_5 = 1$ and $\nu_6 = 1$ states. Levels ~~undergoing to~~ split by asymmetry, ~~splitting,~~ observed for transitions with $K_a \leq 4$, have been denoted with even (K_a+K_c=J) and odd (K_a+K_c=J+1). The unsplit lines have been assigned only once and identified as even transitions. When the first assignments were consistently

Deleted: cm-1
Deleted: 14μm 800 cm-1
Deleted: Ref
Deleted: 6
Deleted: General remarks
Deleted: spatial
Deleted: in
Deleted: bands
Deleted: In this case
Deleted: the fundamental
Deleted: s
Deleted: bands
Deleted: 9
Deleted: later on
Deleted: ,
Deleted: , with perturbation operators.
Deleted: with non diagonal terms responsible for the observed interactions
Deleted: .
Deleted: In addition a number of
Deleted: ν_6=2
Deleted: ′
Deleted: ′
Deleted: ′

checked for each band, the analysis was efficiently assisted by means of computer graphical plots, early proposed by Nakagawa and Overend [11]. They predict transition wavenumbers for each subbranch related to the above mentioned selection rules and involving the same K_a' sublevel. The summary of assignment of the investigated bands is collected in table 1. A complete list of the assigned transitions is available upon request from one of the authors (R.V.)

4 Spectral analysis

The ν_9 band. This fundamental, associated to the C-D/CH_2 out of plane bend mode, is a typical *c*-type band, with very strong $^{P,R}Q$ peaks and comparatively weak P and R features. The low resolution survey spectrum is shown in figure 1 where, just as in a perpendicular band, the successive Q subbranches, evenly spaced of approximately $2(A-\bar{B}) \cong 7.2$ cm^{-1}, are labelled. The identification of the pronounced $^{P,R}Q_K(J)$ clusters is obvious, being the anomalous intensity of the peaks near the band centre due to the effect of asymmetry splitting in the lower K_a quantum numbers. At high resolution the rovibrational structure of the $^{P,R}Q_K(J)$ subbranches is fully resolved. Within each K_a manifold the sequence degrades to lower wavenumbers as the J value increases. The only exception concerns the odd $^{P}Q_1(J)$ multiplet where, as illustrated in figure 2, the sequence degrades from lower to higher wavenumbers up to J = 30 and then reverses the direction.

The P- and R-branch transitions widely spread out all over the large spectral region investigated (890-1090 cm^{-1}). The structure of the $^{P}P_K$ and $^{R}R_K$ subbranches is clear and within each sequence the J lines are separated by $2\bar{B} \cong 0.82$ cm^{-1}. The weaker ^{R}P and ^{P}R transitions with low K_a values have also been identified and subsequently included in the data set.

The ν_3 band. This fundamental corresponds to the CH_2 scissor mode. The low resolution spectrum of figure 3 shows the presence of an hybrid band where the *b*-type structure predominates. The central peak is indicative of the superimposed $^{Q}Q_K(J)$ subbranches (*a*-type) whereas the other prominent peaks refer to the $^{P,R}Q_K(J)$ manifolds (*b*-type).

The high resolution analysis was first devoted to the stronger *b*-type component. The assigned lines cover the spectral range 1320-1560 cm^{-1} reaching, in the R branch, the K_a value

Deleted: 10
Deleted: ;…t ... [1]
Deleted: Spectral analysis
Deleted: (A")
Deleted: ¶ located in the 10μm 990 cm 1 region is and ... [2]
Deleted: of the molecule
Deleted: …just as in a perpendicular band, … …se ... [3]
Deleted: the
Deleted: .
Deleted: for …. From the measured Q-peaks, showing a separation corresponding to 2(A-B⁻) = 7.2 ± 0.3 cm-1 where B⁻ = (B+C)/2, approximated upper state rotational parameters were obtained from a polynomial fit. ... [4]
Deleted: a… both in the P- and R-branches ... [5]
Deleted: ….J-assignment increases moving to lower wavenumbers …with the only exclusion of ... [6]
Deleted: subbbranch
Deleted: which degrades on the opposite side up to J=30 and then reversing the direction as illustrated in figure. 2…The structure attributed to the $^{p}P_{Ka}$ and $^{r}R_{Ka}$ transitions, sequentially located with the approximate separation given by 2B⁻ = 0.82 cm-1, is widely spread all over the large spectral region investigated (890-1090 cm^{-1}). The weaker $^{r}P_{Ka}$ and $^{p}R_{Ka}$ lines for low Ka quantum numbers were also observed and included in the final data set. ... [7]
Deleted: p…r ... [8]
Deleted: for transitions with the same K′a, …, of the strongest ^{p}P and ^{r}R subbranches… ... [9]
Deleted: ¶ (A') ... [10]
Deleted: ¶ , appearing located in the 1435 cm^{-1} 7.0μm region, ... [11]
Deleted: of the molecule…survey shown in …reveals ... [12]
Deleted:
Deleted: In the same figure the
Deleted: .…. ... [13]
Deleted: Concerning to further additional absorptions originating ... [14]
Deleted: On the whole the process of assignment was that described fo ... [15]
Deleted: performed for… ... [16]
Deleted: devoted to …between ... [17]
Deleted: a

of 14. In the P-branch wing the transitions merge into the R branch of the moderately stronger and nearly coincident ν_4 and ν_8 bands. On the whole the rotational structure is well resolved with the exclusion of some subbranches ~~undergoing to~~ split by asymmetry. ~~splitting.~~ Beginning with $K_a \geq 3$, the $^{P,R}Q_K(J)$ multiplets show regularly spaced lines all degrading through the blue. The assignment was checked in many cases by transitions coming from several subbranches and further confirmation was altogether provided when the weaker rotational structure belonging to the *a*-type band was interpreted. Concerning this component, the $^{Q}P(J)$ and $^{Q}R(J)$ subbranches with $J \leq 25$ form, apart the asymmetry splitting of the low K_a values, an almost overlapped structure. An example is given in figure 4, where the lines of the $^{Q}R_K(22,23)$ clusters are labelled. At increasing J values the progression in K_a proceeds regularly towards the blue in both branches. Otherwise, the Q branch also degrading to the blue displays almost completely unresolved features.

During the assignment systematic deviations between predictions and experimental values were very soon manifest and all the K_a sublevels of ν_3 turned out to be, to more or less extent, involved in resonance with the nearby vibrational levels. Among them the only one close in energy is $2\nu_6$ (A′). As known, vibrational anharmonic ($\Delta K_a = 0, \pm 2$) and *c*-type Coriolis ($\Delta K_a = \pm 1, \pm 3$) resonances may occur between levels of the same symmetry species in the C_s group. Assuming for the upper states of ν_3 and $2\nu_6$ the same constants of the ground state, calculations of the rovibrational energy levels indicate that interaction with crossing occurs through first-order *c*-type Coriolis resonance. A peculiar characteristic concerns the transitions reaching the even and odd sublevels with $K_a = 2$. ~~The relative~~ These lines show large displacements from the predicted values and in proximity of the level crossing their intensity drastically decrease giving origin to additional spectral features. They were identified as perturbation-allowed transitions of the $2\nu_6$ overtone, predicted at 1419.2 cm^{-1} and too weak to be detected in the ν_3 spectral region. The avoided crossings were found at J′= 16/17, between $K_a' = 2$ even of ν_3 and $K_a' = 3$ odd of $2\nu_6$, and J′=17/18, between $K_a' = 2$ odd of ν_3 and K_a'= 3 even of $2\nu_6$. A total of 100 lines with J = 12-21 were assigned to the perturber. These interaction effects are pointed out in the spectral portion of figure 5 where it is worth noting the intensity transfer from ν_3 to $2\nu_6$ near the crossing. In particular, the structure of the ν_3 $^{R}Q_1(J)$ manifolds is depicted in the middle and lower panels. A number of perturbation allowed transitions of $2\nu_6$, following the selection rules $\Delta K_a = 2$ and $\Delta K_c = -1$, −3, are illustrated in the upper and lower panels.

Deleted:

Deleted: ν_4 and ν_8 bands,

Deleted: the moderately stronger ν_4/ν_8 band system whose levels are nearly accidental degenerate

Deleted: ¶
T ... [18]

Deleted: "…$^{P,r,\ldots}{}_{a}$ ... [19]

Deleted: ¶
At high resolution the $^{P,R}Q_K(J)$ cluster structure is well resolved and show regularly spaced lines all degrading through the blue, with the exception of with $K_a'' < 3$ subbranches undergoing the asymmetry splitting. ?????¶
the *a*-type…$^{P\ldots R\ldots}$… where the asymmetry splitting is observed for $K_a \leq 3$…shown…wo consecutive clusters…J…with J″=22 and 23, …blue-degrading …. The assignment of the *b*-type component was checked in many cases by transitions coming from several subbranches and further confirmation was altogether provided by the weaker rotational structure of the -type component.¶
The assignment was checked in many cases by transitions coming from several subbranches and further confirmation was altogether provided by the weaker rotational structure of the a-type component. In this case the asymmetry splitting was observed for $Ka'' \leq 3$. In the P- and R-branches up to J< 25, the Ka transitions form an almost overlapped structure; then they originate single lines moving towards higher wavenumbers. An example of this structure is given in figure 4 where two consecutive $^{Q}P_{Ka}(J)$ manifolds are labelled. The Q-branch region, also degrading to the blue, is almost completely unresolved. ... [20]

Deleted: As mentioned the transitions reaching the even and odd sublevels with $K_a'=2$ manifest the stronger effects of perturbation. They showed large displacements from the predicted values and the relative lines drastically decrease the intensity in proximity of the level crossing by partially sharing their strength to the perturbation-allow ... [21]

Deleted: The assignment was checked in many cases by transitions coming from several subbranches and further confirmation was altogether provided by the weaker rotational structure of ... [22]

Deleted: An example of line sequence of the even and odd $^{r}Q_1(J)$ subbranches of ν_3 and the observed lines attributed to the perturber 2v6 is provided in figure 5. (vale un diagramma energetico?) ... [23]

Deleted: Significant irregularities due to …are…, near the crossing, …(even component) …(odd component) ... [24]

Deleted: -

Deleted: (for the even and odd component, respectively),

The $2\nu_6-\nu_6$ and $\nu_5+\nu_6-\nu_5$ hot bands. As mentioned before, the interpretation of their rotational structure was motivated by the fact that the upper states, in particular v_6=2, are involved in the interaction with v_3=1. The assignment was first provided by intensity considerations (the expected intensity relative to ν_6 at room temperature is 6.4% for $2\nu_6-\nu_6$ and 2.5% for $\nu_5+\nu_6-\nu_5$) and by comparison between experimental and calculated anharmonic constants obtained using Gaussian 03 program [12] at the MP2 / 6-311++G (3df, 2pd) level. Due to perturbation, the $2\nu_6-\nu_6$ structure spreads out more rapidly than that of ν_6 and, when not overlapped by the fundamental, a line by line assignment could be achieved. Conversely, the weaker $\nu_5+\nu_6-\nu_5$ shows an almost unresolved structure of the P, Q and R branches. The spectral portion reproducing the $^{Q}P_K$ (23, 24) clusters of $2\nu_6-\nu_6$ and the $^{Q}P_K$(28) multiplet of $\nu_5+\nu_6-\nu_5$ is reported in figure 6. The comparison with the $^{Q}P_K$(32) cluster of ν_6 underlines the different strength with respect to the hot bands. In the same figure it is also interesting to observe the anomalous line sequence in each manifold of $2\nu_6-\nu_6$, in particular the displacement of the features with K_a = 3 due to perturbation with v_3 = 1. The assignment, initially based on lower state combination differences involving R- and P-branch transitions, was later completed with the Q-branch features. For $2\nu_6-\nu_6$ a further check was performed employing the perturbation-allowed transitions of $2\nu_6$ observed in the ν_3 band region.

5. Results

5.1. *The spectroscopic constants of the ground, v_5 = 1 and v_6 = 1 states*

The early ground state constants [7] were determined by mainly forming GSCDs from *a*-type transitions (ΔK_a = 0) of the ν_5 and ν_6 bands. From the present analysis, using *a*- and *b*-type transitions of ν_3 and *c*-type transitions of ν_9, a set of combination differences with ΔK_a = ±1, ±2 can be obtained. The ground states combination differences were weighted, according to the number of transitions sharing a common upper level and, more in detail, they were weighted with the reciprocal of the number of differences carried out in each group using the same procedure described in [13]. A great number of combinations-differences coming from blended lines was discarded. About 5600 combinations, from the four fundamental bands, were taken into account for the determination of the ground state constants given in column

Deleted: ¶
hot ... [25]
Deleted: ¶
Deleted: rotational
Deleted: of these $2\nu_6$ - ν_6 and $\nu_5 + \nu_6$ - ν_5 hot bands …. The expected intensity relative to ν_6 at room temperature is 6.4% for $2\nu_6$ - ν_6 and 2.5% for $\nu_5 + \nu_6$ - ... [26]
Deleted: ir
Deleted: discrimination between the two hot bands…and …the ... [27]
Deleted: when
Deleted: …re ... [28]
Deleted: band
Deleted: n…almost complete combination …$^{q}P_{Ka}$(J), $^{Q}R_{Ka}$ (J) clusters…the two consecutive …a… with J=23 and 24 …As can be seen,…strongest …$^{Q}P_K$(32), ... [29]
Deleted: The comparison with the intermediate multiplet of ν_6
Deleted: of …s compared to the fundamental…and…,…'…effect ... [30]
Deleted: For $2\nu_6$ - ν_6 it can be clearly seen the anomalous sequence of lines belonging to the Ka values, in particular those attributed to the even and odd sublevels with Ka=3 which attain to the upper sublevels undergoing to the major resonance effect with ν_3. …between … transitions ... [31]
Deleted: in the assignment
Deleted: with
Deleted: and assigned to $2\nu_6$.
Deleted: Di $\nu_5 + \nu_6 - \nu_5$ si inizia a parlare e poi resta in sospeso ¶
Deleted: ¶
Deleted: The spectroscopic constants of the ground, v_5= 1 and v_6= 1 states ¶
Deleted: previously lately …using obtained …bands [6] and mainly formed by derived from *a*-type transition ... [32]
Deleted: study of ν_3 (hybrid a- ... [33]
Deleted:
Deleted: with
Deleted: has
Deleted: can also be implemen ... [34]
Deleted: formed … as in [6] ... [35]
Deleted: that is
Deleted: according to
Deleted: using …ref. ... [36]
Deleted: used …present GSCD ... [37]
Deleted: More than 4600 GSC ... [38]
Deleted: ¶ ... [39]

two of table 2. The residuals showed displacements less than 0.0020 cm^{-1} and the standard deviation of the fit (0.541 x 10^{-3} cm^{-1}) is well below the estimated accuracy of measurements. A comparison with the previous values [7], reported for completeness in the first column of table 2, shows that the *A* rotational constant has been greatly improved, whereas the *B* and *C* constants have been determined with an accuracy of about one order of magnitude higher. The values of the five centrifugal distortion constants have also been obtained with better accuracy and agree within two times the early quoted uncertainties. The sextic distortion parameters could not be determined with physical meaning and therefore were constrained to zero.

By fixing the up to date ground state constants, more reliable spectroscopic parameters of v_5=1 and v_6=1 together with the interacting terms were obtained. The results, also included in table 2, were achieved with the same model and data set used in the previous study [7]. As for the ground state, the *A* rotational constant has been greatly improved in the accuracy for both levels whereas the other rotational and centrifugal distortion constants have been optimized. The *c*-type Coriolis and the high-order anharmonic coupling term values remained unaffected.

5.2. *The v_9 = 1 state parameters*

The data were fitted according to a model for an unperturbed rovibrational state. In the least-squares analysis an uncertainty of 0.0010 cm^{-1} was attributed to lines assigned as single transitions. For blended and very weak features the uncertainty was 0.0015 and 0.0020 cm^{-1}, respectively. The fitting procedure was performed using the SPFIT program written by Pickett [14]. With the ground state parameters constrained at the present values of table 2 and employing the full set of assigned transitions, the upper state constants were determined up to the quartic coefficients. The results, reported in table 3, have to be considered satisfactory. The standard deviation is well beyond the experimental uncertainty of measurements and approaches that obtained for the ground and the interacting v_5=1 and v_6=1 states. The comparison between the excited and ground states constants shows very small changes in the centrifugal distortion parameters so pointing out the absence of perturbations.

5.3. *The v_3 = 1, v_6 = 2 and v_5 = v_6 = 1 state parameters*

Deleted: using 5000 GSCDs which
Deleted: in the residuals. The
Deleted: The
Deleted:
Deleted: of ref.
Deleted: 6
Deleted: work [6]
Deleted: value
Deleted: .
Deleted: values
Deleted: they
Deleted: at the values of table 2
Deleted: can also be
Deleted: by adopting
Deleted: work
Deleted: 6
Deleted: and using the early data set
Deleted: in the absolute value as well as
Deleted: The
Deleted: and
Deleted: parameters
Deleted: constants
Deleted: also
Deleted: in their absolute values
Deleted:
Deleted: whereas
Deleted: experimental
Deleted: s Unitary weights were given to unblended features whereas, w ... [40]
Deleted:
Deleted: Systematic deviations ... [41]
Deleted: to
Deleted: , whereas
Deleted: f
Deleted: and
Deleted:
Deleted: and
Deleted: , respectively
Deleted: fixed
Deleted: ,
Deleted: have been
Deleted: obtained from the fit,
Deleted: evaluation of the
Deleted: to
Deleted: of the excited state co ... [42]

The initial spectroscopic constants were provided from preliminary single band fits by selecting the apparently less perturbed transitions. The same procedure described for ν_9 was adopted for the evaluation of the uncertainties concerning the ν_3, $2\nu_6$ and $2\nu_6 - \nu_6$ data, while for $\nu_5 + \nu_6 - \nu_5$ the uncertainty of 0.004 cm^{-1} was assumed. The upper states belong to the same vibrational symmetry species, hence the interactions, besides the *c*-type Coriolis ($E^{\pm} \leftrightarrow O^{\mp}$), can also occur through anharmonic ($E^{\pm} \leftrightarrow E^{\pm}$, $O^{\pm} \leftrightarrow O^{\pm}$) resonance. At first, only transitions with low K_a and medium J values were used in a simultaneous treatment. The upper state rotational levels were calculated including in the Hamiltonian the *c*-type Coriolis and Fermi operators:

$$\boldsymbol{H}^{c}_{3,66} = \mathrm{i}\,\xi^{c}_{3,66}\,\boldsymbol{P}_c.$$

$$\boldsymbol{H}^{anh}_{3,66} = W_{3,66}$$

The lower state parameters were constrained at the values of table 2. Subsequently the body of data was gradually enlarged with all the assigned transitions of the above-mentioned bands and those involving $\nu_5 + \nu_6 - \nu_5$. Large discrepancies for high K_a values of ν_3 were obtained between calculated and experimental wavenumbers. Despite the several attempts performed to fit the data with different choices of the refined parameters, the quality and the number of the resulting spectroscopic constants remained unaltered. Considering the course of the residuals and an approximate energy level diagram it can be assumed that the next closer vibrational states $v_4 = 1$ (A′) and $v_8 = 1$ (A″) should be responsible for the large discrepancies observed for the high K_a stacks of ν_3.

The final set of spectroscopic constants was then obtained using 2942 transitions of ν_3 with $K_a' \leq 9$ and the full set of the $2\nu_6$ and $2\nu_6 - \nu_6$ data. The resulting effective spectroscopic parameters are summarized in table 3. As shown the rotational constants and the coupling terms connecting the interacting levels are well determined. The Δ_J and Δ_{JK} diagonal centrifugal distortion values are in satisfactory agreement with those of the ground state, while Δ_{JK} slightly differs on opposite direction for the v_3=1 and v_6=2 levels, suggesting that additional interactions should be considered. The higher standard deviation, compared to that obtained for ν_9 and ν_5/ν_6, mainly derives from the systematic deviations in the residuals of ν_3 for transitions with K_a= 7-9 at high J values.

Since the transitions involving $v_5 = v_6 = 1$ were excluded from the previous calculations, they were fitted separately by assuming the model for an unperturbed band. The results, also included in table 3, were derived by the constraint of the centrifugal distortion constants to those of the $v_5 = 1$, since their release ~~unaffected~~ did not affect the standard deviation of the fit. The lower degree in the accuracy of the determined spectroscopic constants is mainly depending on the quality and the number of assigned lines which account, as noted above, for a most unresolved rotational structure in the hot band lines.

6. Discussion and conclusion

Spectral simulations based on the spectroscopic parameters given in table 2 and 3 were performed in different spectral regions of the ν_3 band in order to establish the dipole moment ratio along the *a* and *b* axis. The SPCAT program [14] was used to predict line positions and intensities. A reasonable agreement between experimental and synthetic spectrum was obtained with the ratio $|\Delta\mu_a/\Delta\mu_b| = 0.45 \pm 0.05$. Besides, considering the band origins of ν_3 and $2\nu_6$ and the Fermi interaction term (see table 3) the shift of the interacting vibrational levels was calculated to be $|1.545|$ cm^{-1}.

A number of parameters can be compared with quantum-mechanical calculations. The vibration-rotation interactions constants α of the considered fundamentals are given in table 4 together with the values calculated *ab initio*, using Gaussian 03 program [12]. The predictions are in satisfactory agreement except for α_A of ν_3 which considerably differs from the experimental value. The discrepancy can be attributed to additional resonances with the ν_4 and ν_8 levels, which should play a significant role. Another explanation relies with the calculated value obtained without taking into account the interaction of ν_3 with the near fundamental levels. This last point suggests that calculated values for rovibrational prediction of bands, when strong resonances are expected to occur, should be taken with care.

From the vibrational levels of $v_5 = 1$, $v_6 = 1$, $v_6 = 2$ and $v_5 = v_6 = 1$, the anharmonicity constants $x_{56} = -4.289$ cm^{-1} and $x_{66} = -3.634$ cm^{-1} have been derived and can be compared with the values of -4.281 cm^{-1} and -2.745 cm^{-1}, respectively, calculated *ab initio* [12].

While the ν_9 band has been fully interpreted, a deeper understanding of the ν_3 spectral region needs the analysis of the complex band system involving $v_4 = 1$ and $v_8 = 1$, and higher

Deleted: calculated
Deleted: three
Deleted: The
Deleted: As shown
Deleted: t
Deleted: obtained
Deleted: com
Deleted: prehensive fit occurring in
Deleted: would
Deleted: require an
Deleted: extended
Deleted: *the*
Deleted: states
Deleted: the assignment

quality spectra to better characterize the $v_6 = 2$ and $v_5 = v_6 = 1$ states. Nevertheless more accurate ground state constants, including the set of centrifugal distortion constants up to higher orders, should require measurements in the microwave and/or in the IR region with powerful Fourier transform spectrometers.

Deleted: further rovibrational transitions

Deleted: improved

Deleted: would necessitate

Acknowledgements

This work has been supported by PRIN funds (project "Trasferimenti di energia e di carica a livello molecolare") and by University of Venice (FRA funds). The authors gratefully acknowledge A. Baldan for the synthesis of the sample and for bibliographic support.

References

[1] R. Nassar, P. F. Bernath, C. D. Boone, C. Clerbaux, P.F. Coheur, G. Dufour, L. Froidevaux, E. Mahieu, J. C. McConnell, S. D. McLeod, D. P. Murtagh, C. P. Rinsland, K. Semeniuk, R. Skelton, K. A. Walker, R. Zander, J. Geophys. Res., 111, D22312 (2006).

[2] D. Jacquemart, F. Kwabia Tchana, N. Lacome, I. Kleiner, J. Quant. Spetrosc.& Rad. Transfer, 105, 264 (2007).

[3] M. Litz, H. Burger, L. Fejiard, F.L. Constantin, L. Margules, J. Demaison, J. Mol. Spectrosc., 219, 238 (2003).

[4] F. L. Constantin, J. Demaison, L. Fejiard, M. Litz, H. Burger, P. Pracna, Mol. Phys., 102, 1717 (2004).

[5] G. M. Black and M. M. Law, J. Mol. Spectrosc., 205, 280 (2001).

[6] J. R. Riter, D. F. Eggers, J. Chem. Phys., 44, 745 (1966).

[7] A. Baldacci, P. Stoppa, A. Pietropolli Charmet, S. Giorgianni, G. Nivellini, Mol. Phys., 103, 2803-2811 (2005).

[8] J. M. Orza, C. Domingo, R. Escribano, S. Montero, J. Raman Spectrosc., 10, 215- 220 (1981).

[9] G. Guelachvili and K. Narahari Rao, "Handbook of Infrared Standards", Academic Press, London, 1986.

[10] J. K. Watson, "Vibrational Spectroscopy and Structure", Vol. 6, J. R. Durig, (Ed.), pp 1-89, Elsevier, Amsterdam, (1977).

[11] T. Nakagawa, J. Overend, J. Mol. Spectrosc., 50, 333 (1974).

[12] Gaussian 03, Revision A.1, M. J. Frisch, G. W. Trucks, H. B. Schlegel, G. E. Scuseria, M. A. Robb, J. R. Cheeseman, J. A. Montgomery, Jr., T. Vreven, K. N. Kudin, J. C. Burant, J. M. Millam, S. S. Iyengar, J. Tomasi, V. Barone, B. Mennucci, M. Cossi, G. Scalmani, N. Rega, G. A. Petersson, H. Nakatsuji, M. Hada, M. Ehara, K. Toyota, R. Fukuda, J. Hasegawa, M. Ishida, T. Nakajima, Y. Honda, O. Kitao, H. Nakai, M.

Deleted: 7

Deleted: 6

Deleted: 11

Deleted: 8

Deleted: 9

Deleted: 10

Klene, X. Li, J. E. Knox, H. P. Hratchian, J. B. Cross, C. Adamo, J. Jaramillo, R. Gomperts, R. E. Stratmann, O. Yazyev, A. J. Austin, R. Cammi, C. Pomelli, J. W. Ochterski, P. Y. Ayala, K. Morokuma, G. A. Voth, P. Salvador, J. J. Dannenberg, V. G. Zakrzewski, S. Dapprich, A. D. Daniels, M. C. Strain, O. Farkas, D. K. Malick, A. D. Rabuck, K. Raghavachari, J. B. Foresman, J. V. Ortiz, Q. Cui, A. G. Baboul, S. Clifford, J. Cioslowski, B. B. Stefanov, G. Liu, A. Liashenko, P. Piskorz, I. Komaromi, R. L. Martin, D. J. Fox, T. Keith, M. A. Al-Laham, C. Y. Peng, A. Nanayakkara, M. Challacombe, P. M. W. Gill, B. Johnson, W. Chen, M. W. Wong, C. Gonzalez, and J. A. Pople, Gaussian, Inc., Pittsburgh PA, 2003.

[13] F. Hegelund, H. Burger, O. Polanz, J. Mol. Spectrosc., 181, 151 (1997).

[14] H. M. Pickett, J. Mol. Spectrosc., 148, 371 (1991).

Figure captions

Figure 1. Overview of the low resolution (0.5 cm^{-1}) IR spectrum of $CH_2D^{35}Cl$ ν_9 fundamental (P = 4 kPa, room temperature, 10 cm cell). The contour is typical of an unperturbed *c*-type band of a near prolate asymmetric top. The high resolution spectrum of the central peak marked with * is reproduced in Fig. 2.

Figure 2. Details of the fine structure of the odd $^{P}Q_1(J)$ multiplet of $CH_2D^{35}Cl$ ν_9 fundamental (path length 5 m, P = 173 Pa).

Figure 3. Overview of the low resolution (0.5 cm^{-1}) IR spectrum of $CH_2D^{35}Cl$ ν_3 fundamental (P = 4 kPa, room temperature, 10 cm cell). The contour is indicative of an hybrid *a*/*b*-type band of a near prolate asymmetric top where the *b*-type component predominates. The assignment of the resolved rotational structure of the broad peak marked with * is reported in Fig 4.

Figure 4. Spectral portion of $CH_2D^{35}Cl$ ν_3 fundamental (path length 5 m, P = 40 Pa) showing the structure of the *a*-type lines for the $^{Q}R_K(22,23)$ multiplets. Asymmetry splitting is observed for K_a = 1, 2.

Figure 5. Details of the spectrum of $CH_2D^{35}Cl$ ν_3 fundamental (path length 5 m, P = 40 Pa) showing the assignment of the even/odd $^{R}Q_1(J)$ subbranches (*b*-type component) and even/odd $^{S}Q_1(J)$ perturbation-allowed transitions of $2\nu_6$, observed in proximity of the level crossings.

Figure 6. Spectral portion of $CH_2D^{35}Cl$ of the ν_6 fundamental region (path length 15 cm, P = 150 Pa) showing the $^{Q}P_K(23,24)$ multiplets of $2\nu_6-\nu_6$ and $^{Q}P_K(28)$ of $\nu_5+\nu_6-\nu_5$, denoted with *. The former hot band shows an almost complete resolved rotational structure, while the latter one originates a broad peak feature accounting for the same J and different K_a values. The $^{Q}P_K(32)$ cluster of ν_6 is also indicated.

Page 6: [1] Deleted Raffaella Visinoni 2/8/2008 11:10:00 AM
;

Page 6: [1] Deleted Raffaella Visinoni 2/8/2008 11:10:00 AM
t

Page 6: [2] Deleted Agostino Baldacci 2/9/2008 11:36:00 AM

Page 6: [2] Deleted Agostino Baldacci 2/9/2008 11:37:00 AM
located in the 10μm 990 cm ^{1} region is and

Page 6: [3] Deleted Agostino Baldacci 2/11/2008 10:07:00 AM

Page 6: [3] Deleted Agostino Baldacci 2/11/2008 10:07:00 AM
just as in a perpendicular band,

Page 6: [3] Deleted Agostino Baldacci 2/11/2008 12:59:00 PM

Page 6: [3] Deleted Agostino Baldacci 2/11/2008 12:59:00 PM
se

Page 6: [4] Deleted Raffaella Visinoni 1/31/2008 1:07:00 PM
for

Page 6: [4] Deleted Raffaella Visinoni 2/11/2008 3:31:00 PM
. From the measured Q-peaks, showing a separation corresponding to 2(A-B^{-}) = 7.2 ± 0.3 cm-1 where B^{-}= (B+C)/2, approximated upper state rotational parameters were obtained from a polynomial fit.

Page 6: [5] Deleted Agostino Baldacci 2/9/2008 11:38:00 AM
a

Page 6: [5] Deleted Agostino Baldacci 2/9/2008 11:42:00 AM
both in the P- and R-branches

Page 6: [6] Deleted Raffaella Visinoni 2/11/2008 3:31:00 PM
.

Page 6: [6] Deleted Raffaella Visinoni 1/31/2008 1:42:00 PM
J-assignment increases moving to lower wavenumbers

Page 6: [6] Deleted Raffaella Visinoni 1/31/2008 1:45:00 PM
with the only exclusion of

Page 6: [7] Deleted Raffaella Visinoni 1/31/2008 1:48:00 PM

which degrades on the opposite side up to J=30 and then reversing the direction as illustrated in figure. 2

Page 6: [7] Deleted **Raffaella Visinoni** **2/4/2008 12:58:00 PM**

The structure attributed to the $^{p}P_{Ka}$ and $^{r}R_{Ka}$ transitions, sequentially located with the approximate separation given by $2B^{-}$ = 0.82 cm-1, is widely spread all over the large spectral region investigated (890-1090 cm^{-1}). The weaker $^{r}P_{Ka}$ and $^{p}R_{Ka}$ lines for low Ka quantum numbers were also observed and included in the final data set.

Page 6: [8] Deleted **Raffaella Visinoni** **2/11/2008 3:34:00 PM**

p

Page 6: [8] Deleted **Raffaella Visinoni** **2/11/2008 3:34:00 PM**

r

Page 6: [9] Deleted **Agostino Baldacci** **2/11/2008 10:13:00 AM**

for transitions with the same K'_a,

Page 6: [9] Deleted **Agostino Baldacci** **2/11/2008 10:13:00 AM**

, of the strongest ^{p}P and ^{r}R subbranches

Page 6: [9] Deleted **Agostino Baldacci** **2/11/2008 10:13:00 AM**

Page 6: [10] Deleted **Raffaella Visinoni** **2/8/2008 1:31:00 PM**

Page 6: [10] Deleted **Raffaella Visinoni** **2/7/2008 2:24:00 PM**

(A')

Page 6: [11] Deleted **Agostino Baldacci** **2/9/2008 11:44:00 AM**

Page 6: [11] Deleted **Agostino Baldacci** **2/9/2008 11:45:00 AM**

, appearing located in the 1435 cm^{-1} 7.0μm region,

Page 6: [12] Deleted **Raffaella Visinoni** **2/4/2008 2:15:00 PM**

of the molecule

Page 6: [12] Deleted **Raffaella Visinoni** **2/8/2008 1:32:00 PM**

survey

Page 6: [12] Deleted **Raffaella Visinoni** **2/8/2008 1:32:00 PM**

shown in

Page 6: [12] Deleted **Raffaella Visinoni** **2/8/2008 1:32:00 PM**

reveals

Page 6: [13] Deleted Agostino Baldacci 2/11/2008 10:14:00 AM

a

Page 6: [13] Deleted Agostino Baldacci 2/11/2008 10:14:00 AM

a

Page 6: [14] Deleted Raffaella Visinoni 2/5/2008 4:50:00 PM

Concerning to further additional absorptions originating from the ground state, the overtone $2\nu_6$ is predicted at 1419.2 cm-1. The survey spectrum does not show any other prominent feature. This point suggests that, if present, $2\nu_6$ should be very weak as usually happens for overtone or combinations when the resonance effect is not accompanied by transfer of intensity from the light state to the closer dark one.

Page 6: [15] Deleted Raffaella Visinoni 2/8/2008 3:16:00 PM

On the whole the process of assignment was that described for ν_9. The important difference is that ν_3 is globally interacting. As a consequence the predicted transitions based on spectroscopic constants for unperturbed bands showed systematic deviations from the calculated values. The perturbation manifests a peculiar characteristic for transitions with low Ka values in the excited state but, to more or less extent, all the Ka sublevels of ν_3 are involved by resonance with the nearby vibrational levels.

Page 6: [16] Deleted Agostino Baldacci 2/9/2008 11:46:00 AM

performed for

Page 6: [16] Deleted Agostino Baldacci 2/9/2008 11:46:00 AM

Page 6: [17] Deleted Raffaella Visinoni 2/4/2008 5:18:00 PM

devoted to

Page 6: [17] Deleted Raffaella Visinoni 2/4/2008 5:18:00 PM

between

Page 6: [17] Deleted Raffaella Visinoni 2/4/2008 5:21:00 PM

Page 7: [18] Deleted Agostino Baldacci 2/9/2008 11:49:00 AM

Page 7: [18] Deleted Agostino Baldacci 2/9/2008 11:49:00 AM

T

Page 7: [19] Deleted Raffaella Visinoni 2/11/2008 3:35:00 PM
,,

Page 7: [19] Deleted Raffaella Visinoni 2/11/2008 3:35:00 PM
p,r

Page 7: [19] Deleted Raffaella Visinoni 2/11/2008 3:35:00 PM
a

Page 7: [20] Deleted Agostino Baldacci 2/11/2008 11:04:00 AM

At high resolution the $^{P,R}Q_K(J)$ cluster structure is well resolved and show regularly spaced lines all degrading through the blue, with the exception of with $K_a'' < 3$ subbranches undergoing the asymmetry splitting. ?????

Page 7: [20] Deleted Agostino Baldacci 2/11/2008 11:06:00 AM
the *a*-type

Page 7: [20] Deleted Agostino Baldacci 2/11/2008 10:25:00 AM
P

Page 7: [20] Deleted Agostino Baldacci 2/11/2008 10:25:00 AM
R

Page 7: [20] Deleted Agostino Baldacci 2/11/2008 10:30:00 AM

Page 7: [20] Deleted Agostino Baldacci 2/11/2008 10:39:00 AM
where the asymmetry splitting is observed for $K_a \leq 3$

Page 7: [20] Deleted Agostino Baldacci 2/11/2008 11:11:00 AM
shown

Page 7: [20] Deleted Agostino Baldacci 2/11/2008 10:29:00 AM
wo consecutive clusters

Page 7: [20] Deleted Agostino Baldacci 2/11/2008 10:28:00 AM
J

Page 7: [20] Deleted Agostino Baldacci 2/11/2008 10:28:00 AM
with J″=22 and 23,

Page 7: [20] Deleted Agostino Baldacci 2/11/2008 11:15:00 AM
blue-degrading

Page 7: [20] Deleted Agostino Baldacci 2/11/2008 11:16:00 AM

. The assignment of the *b*-type component was checked in many cases by transitions coming from several subbranches and further confirmation was altogether provided by the weaker rotational structure of the -type component.

The assignment was checked in many cases by transitions coming from several subbranches and further confirmation was altogether provided by the weaker rotational structure of the a-type component. In this case the asymmetry splitting was observed for Ka"≤ 3. In the P- and R-branches up to J< 25, the Ka transitions form an almost overlapped structure; then they originate single lines moving towards higher wavenumbers. An example of this structure is given in figure 4 where two consecutive $^{q}P_{Ka}(J)$ manifolds are labelled. The Q-branch region, also degrading to the blue, is almost completely unresolved.

Page 7: [21] Deleted **Raffaella Visinoni** **2/5/2008 5:00:00 PM**

As mentioned the transitions reaching the even and odd sublevels with $K_a'=2$ manifest the stronger effects of perturbation. They showed large displacements from the predicted values and the relative lines drastically decrease the intensity in proximity of the level crossing by partially sharing their strength to the perturbation-allowed transitions of the interacting level $v_6=2$. In total 100 lines belonging to the perturber with Ka'=3 were assigned for J values between 14-21 in either a- and b-type components of v_3.

Page 7: [22] Deleted **Agostino Baldacci** **2/11/2008 11:16:00 AM**

The assignment was checked in many cases by transitions coming from several subbranches and further confirmation was altogether provided by the weaker rotational structure of the a-type component.

Page 7: [22] Deleted **Agostino Baldacci** **2/11/2008 11:21:00 AM**

transferred

Page 7: [22] Deleted **Agostino Baldacci** **2/11/2008 11:22:00 AM**

identified in the spcctrum

Page 7: [22] Deleted **Agostino Baldacci** **2/11/2008 11:35:00 AM**

assigned

Page 7: [22] Deleted **Agostino Baldacci** **2/11/2008 11:17:00 AM**

Page 7: [22] Deleted **Agostino Baldacci** **2/11/2008 11:24:00 AM**

Page 7: [22] Deleted Agostino Baldacci 2/11/2008 11:29:00 AM

(

Page 7: [22] Deleted Agostino Baldacci 2/11/2008 11:36:00 AM

+

Page 7: [22] Deleted Agostino Baldacci 2/11/2008 11:29:00 AM

Page 7: [22] Deleted Agostino Baldacci 2/11/2008 11:36:00 AM

-

Page 7: [22] Deleted Agostino Baldacci 2/11/2008 11:37:00 AM

)

Page 7: [22] Deleted Agostino Baldacci 2/11/2008 11:37:00 AM

(

Page 7: [22] Deleted Agostino Baldacci 2/11/2008 11:38:00 AM

-

Page 7: [22] Deleted Agostino Baldacci 2/11/2008 11:38:00 AM

3^{+}

Page 7: [22] Deleted Agostino Baldacci 2/11/2008 1:02:00 PM

)

Page 7: [22] Deleted Agostino Baldacci 2/11/2008 11:39:00 AM

$K_a' = 3$ and

Page 7: [22] Deleted Agostino Baldacci 2/11/2008 11:40:00 AM

values between

Page 7: [22] Deleted Agostino Baldacci 2/11/2008 11:32:00 AM

Page 7: [23] Deleted Raffaella Visinoni 2/8/2008 11:42:00 AM

An example of line sequence of the even and odd $^{r}Q_1(J)$ subbranches of ν_3 and the observed lines attributed to the perturber 2v6 is provided in figure 5. (vale un diagramma energetico?)The avoided crossings were found at J'= 16/17 for Ka =2 even and Ka = 3 odd, and J= 17/18 for Ka =2 odd and Ka = 3 even of ν_3 and $2\nu_6$, respectively.

Page 7: [24] Deleted Agostino Baldacci 2/9/2008 11:54:00 AM

Significant irregularities due to

Page 7: [24] Deleted	Agostino Baldacci	2/9/2008 11:54:00 AM

are

Page 7: [24] Deleted	Agostino Baldacci	2/9/2008 11:54:00 AM

, near the crossing,

Page 7: [24] Deleted	Agostino Baldacci	2/11/2008 12:13:00 PM

(even component)

Page 7: [24] Deleted	Agostino Baldacci	2/11/2008 12:13:00 PM

(odd component)

Page 7: [24] Deleted	Agostino Baldacci	2/11/2008 11:33:00 AM

Some

Page 8: [25] Deleted	Raffaella Visinoni	2/11/2008 3:36:00 PM

Page 8: [25] Deleted	Raffaella Visinoni	2/7/2008 2:24:00 PM

hot

Page 8: [26] Deleted	Agostino Baldacci	2/11/2008 12:14:00 PM

of these $2\nu_6 - \nu_6$ and $\nu_5 + \nu_6 - \nu_5$ hot bands

Page 8: [26] Deleted	Agostino Baldacci	2/9/2008 12:00:00 PM

. The expected intensity relative to ν_6 at room temperature is 6.4% for $2\nu_6 - \nu_6$ and 2.5% for $\nu_5 + \nu_6 - \nu_5$.

Page 8: [27] Deleted	Agostino Baldacci	2/11/2008 12:20:00 PM

discrimination between the two hot bands

Page 8: [27] Deleted	Agostino Baldacci	2/9/2008 11:59:00 AM

and

Page 8: [27] Deleted	Agostino Baldacci	2/9/2008 12:01:00 PM

the

Page 8: [28] Deleted	Agostino Baldacci	2/9/2008 12:01:00 PM

Page 8: [28] Deleted	Agostino Baldacci	2/9/2008 12:01:00 PM

re

Page 8: [29] Deleted	Agostino Baldacci	2/11/2008 12:22:00 PM

n

Page 8: [29] Deleted	**Agostino Baldacci**	**2/11/2008 12:22:00 PM**

almost complete

Page 8: [29] Deleted	**Agostino Baldacci**	**2/9/2008 12:02:00 PM**

combination

Page 8: [29] Deleted	**Agostino Baldacci**	**2/9/2008 12:02:00 PM**

$^{q}P_{Ka}(J)$, $^{Q}R_{Ka}$ (J) clusters

Page 8: [29] Deleted	**Agostino Baldacci**	**2/9/2008 12:06:00 PM**

the two consecutive

Page 8: [29] Deleted	**Agostino Baldacci**	**2/9/2008 12:03:00 PM**

a

Page 8: [29] Deleted	**Agostino Baldacci**	**2/9/2008 12:04:00 PM**

Page 8: [29] Deleted	**Agostino Baldacci**	**2/11/2008 12:23:00 PM**

with J=23 and 24

Page 8: [29] Deleted	**Agostino Baldacci**	**2/9/2008 12:07:00 PM**

As can be seen,

Page 8: [29] Deleted	**Agostino Baldacci**	**2/11/2008 12:24:00 PM**

strongest

Page 8: [29] Deleted	**Agostino Baldacci**	**2/11/2008 1:05:00 PM**

$^{Q}P_{K}(32)$,

Page 8: [30] Deleted	**Agostino Baldacci**	**2/9/2008 12:07:00 PM**

of

Page 8: [30] Deleted	**Agostino Baldacci**	**2/9/2008 12:08:00 PM**

s compared to the fundamental

Page 8: [30] Deleted	**Agostino Baldacci**	**2/11/2008 12:23:00 PM**

and

Page 8: [30] Deleted	**Agostino Baldacci**	**2/11/2008 12:25:00 PM**

,

Page 8: [30] Deleted	**Agostino Baldacci**	**2/9/2008 12:10:00 PM**

'

Page 8: [30] Deleted	**Agostino Baldacci**	**2/9/2008 12:10:00 PM**

effect

Page 8: [30] Deleted Agostino Baldacci 2/11/2008 12:24:00 PM
level.

Page 8: [31] Deleted Raffaella Visinoni 2/6/2008 12:16:00 PM
For $2\nu_6$ - ν_6 it can be clearly seen the anomalous sequence of lines belonging to the Ka values, in particular those attributed to the even and odd sublevels with Ka=3 which attain to the upper sublevels undergoing to the major resonance effect with ν_3.

Page 8: [31] Deleted Raffaella Visinoni 2/6/2008 12:01:00 PM
between

Page 8: [31] Deleted Raffaella Visinoni 2/8/2008 2:41:00 PM
transitions

Page 8: [32] Deleted Agostino Baldacci 2/11/2008 1:05:00 PM
previously lately

Page 8: [32] Deleted Agostino Baldacci 2/9/2008 12:19:00 PM
using

Page 8: [32] Deleted Agostino Baldacci 2/9/2008 12:17:00 PM
obtained

Page 8: [32] Deleted Agostino Baldacci 2/9/2008 12:21:00 PM
bands [6] and mainly formed by derived from *a*-type transitions ($\Delta K_a = 0$) of ν_5 and ν_6 [6].

Page 8: [32] Deleted Agostino Baldacci 2/11/2008 12:29:00 PM
having

Page 8: [33] Deleted Raffaella Visinoni 2/6/2008 3:19:00 PM
study of ν_3 (hybrid a- and b-type band) and ν_9 (c-type band), GSCDs

Page 8: [34] Deleted Raffaella Visinoni 2/6/2008 4:06:00 PM
can also be implemented and used to provide with greater accuracy the ground state constants in particular those connected with the principal moment of inertia I_a.

Page 8: [35] Deleted Agostino Baldacci 2/11/2008 1:06:00 PM
formed

Page 8: [35] Deleted Agostino Baldacci 2/11/2008 12:30:00 PM
as in [6]

Page 8: [36] Deleted Raffaella Visinoni 2/6/2008 3:28:00 PM
using

Page 8: [36] Deleted Raffaella Visinoni 2/6/2008 3:28:00 PM
ref.

Page 8: [37] Deleted Agostino Baldacci 2/11/2008 12:31:00 PM
used

Page 8: [37] Deleted Agostino Baldacci 2/11/2008 12:32:00 PM
present GSCDs analysis

Page 8: [37] Deleted Agostino Baldacci 2/9/2008 12:23:00 PM
.

Page 8: [38] Deleted Raffaella Visinoni 2/6/2008 4:25:00 PM
More than 4600 GSCDs were available from the four fundamentals for a simultaneous ground state analysis However a great number of combinations-differences, mainly those implying transitions coming from blended lines, were discarded.

Page 8: [39] Deleted Agostino Baldacci 2/9/2008 12:23:00 PM

Page 8: [39] Deleted Agostino Baldacci 2/9/2008 12:23:00 PM
T

Page 8: [39] Deleted Agostino Baldacci 2/9/2008 12:23:00 PM
are

Page 9: [40] Deleted Raffaella Visinoni 2/8/2008 3:02:00 PM
s Unitary weights were given to unblended features whereas, when not rejected, they were reduced by a factor of 2 or 10 for blended and/or weaker lines. The spectroscopic constants, given in table 3, have been determined up to the quartic centrifugal distortion constants. They were obtained from the full set of assigned transitions as reported in table 1.

Page 9: [41] Deleted Raffaella Visinoni 2/6/2008 2:48:00 PM
Systematic deviations in the residuals are absent.

Page 9: [42] Deleted Raffaella Visinoni 2/6/2008 2:53:00 PM
of the excited state constants with the ground state of table 2 shows that the changes in the centrifugal distortion constants are very small. Hence that there is no indication of possible resonances with other vibrational states and therefore the use of an unperturbed model is justified.

Table 1. Summary of assignment of the ν_3, ν_9, $2\nu_6$, $2\nu_6-\nu_6$ and $\nu_5+\nu_6-\nu_5$ bands of $CH_2D^{35}Cl$

	ν_3	ν_9	$2\nu_6$	$2\nu_6-\nu_6$	$\nu_5+\nu_6-\nu_5$
Subbranches	^{Q}P, ^{Q}R $^{P,R}P$, $^{P,R}Q$, $^{P,R}R$	$^{P,R}P$, $^{P,R}Q$, $^{P,R}R$	$^{Q,R,S}P$, $^{Q,S}Q$, $^{Q,R,S}R$	^{Q}P, ^{Q}Q, ^{Q}R	^{Q}P, ^{Q}Q, ^{Q}R
a-type transitions	$0 \le J \le 47$ $0 \le K_a \le 8$		$12 \le J \le 21$ $K_a = 3$	$2 \le J \le 34$ $0 \le K_a \le 10$	$3 \le J \le 29$ $3 \le K_a \le 8$
b-type transitions	$0 \le J \le 52$ $0 \le K_a \le 14$		$15 \le J \le 18$ $K_a = 3$		
c-type transitions		$0 \le J \le 48$ $0 \le K_a \le 12$			
N° of transitions	3616	1898	100	580	148

Table 2. Spectroscopic constants (cm^{-1}) for the ground, $v_5 = 1$ and $v_6 = 1$ states of $CH_2D^{35}Cl$ [a]

	Ground State		$v_5 = 1$	$v_6 = 1$
	Ref. 7	Present work		
ν_0			827.023427(83)	714.112679(87)
A	3.9991(14)	3.9972702(13)	4.0006281(28)	3.9938571(25)
B	0.4162677(13)	0.41626600(25)	0.41450372(52)	0.41328964(36)
C	0.4061849(13)	0.40618709(25)	0.40452555(93)	0.40316713(84)
$\Delta_J \times 10^6$	0.5022(2)	0.502012(70)	0.49443(11)	0.510001(67)
$\Delta_{JK} \times 10^5$	0.5178(3)	0.518580(93)	0.50877(31)	0.52971(26)
$\Delta_K \times 10^4$	0.68(11)	0.543167(62)	0.53566(18)	0.54710(14)
$\delta_J \times 10^7$	0.1234(15)	0.12096(35)	0.0876(12)	0.14045(59)
$\delta_K \times 10^6$	1.1(3)	0.783(40)	0.33(11)	0.790(72)
$\xi^c_{5,6}$			0.16292(27)	
$W_{5,6} \times 10^4$			–0.3857(41)	
$\sigma \times 10^3$	0.427	0.541	0.467	
No. of Data	1486	5635	2100	2526
J max	57	57	52	57
K_a max	14	14	14	14

[a] Quoted uncertainties are one standard deviation in units of the last significant digit.

Table 3. Spectroscopic constants (cm^{-1}) of the $v_3 = 1$, $v_6 = 2$, $v_9 = 1$ and $v_5 = v_6 = 1$ states of $CH_2D^{35}Cl$ [a]

	$v_3 = 1$	$v_6 = 2$	$v_9 = 1$	$v_5 = v_6 = 1$
ν_0	1433.8391(27)	1420.9576(27)	986.690131(64)	1536.84695(54)
A	3.9977994(36)	3.9905199(85)	4.0233803(31)	3.997486(17)
B	0.4166366(12)	0.4102436(14)	0.41517453(34)	0.41060(23)
C	0.4083607(13)	0.3997064(16)	0.40473506(33)	0.40247(23)
$\Delta_J \times 10^6$	0.53478(26)	0.51712(63)	0.50244(13)	0.49443 [b]
$\Delta_{JK} \times 10^5$	0.32042(20)	0.6329(10)	0.56907(32)	0.50877 [b]
$\Delta_K \times 10^4$	0.58649(43)	0.55810(85)	0.58388(24)	0.53566 [b]
$\delta_J \times 10^7$	0.11914(80)	0.12220(99)	0.12899(83)	0.0876 [b]
$\delta_K \times 10^6$	0.782(10)	0.811(10)	0.707(33)	0.33 [b]
$\xi^{c}_{3,66}$	0.0629349(56)			
$W_{3,66}$	4.7216(37)			
$\sigma \times 10^3$	1.57		0.663	2.02
No. of Data	2942	680	1898	148
J_{max}	52	34	48	29
$K_{a\,max}$	9	10	12	8

[a] Quoted uncertainties are one standard deviation in units of the last significant digit.
[b] Fixed to the $v_5 = 1$ state value.

Table 4. Experimental and calculated vibration-rotation interaction constants α (x 10^3 cm^{-1}) for $CH_2D^{35}Cl$

	ν_3		ν_5		ν_6		ν_9	
	Exp.	Calc.	Exp.	Calc.	Exp.	Calc.	Exp.	Calc.
α_A	–0.53	–12.48	–3.36	–3.01	3.41	2.36	–26.11	–24.60
α_B	–0.37	–0.31	1.76	2.00	2.98	2.45	1.09	0.98
α_C	–2.17	–2.28	1.66	1.45	3.02	2.93	1.45	1.42

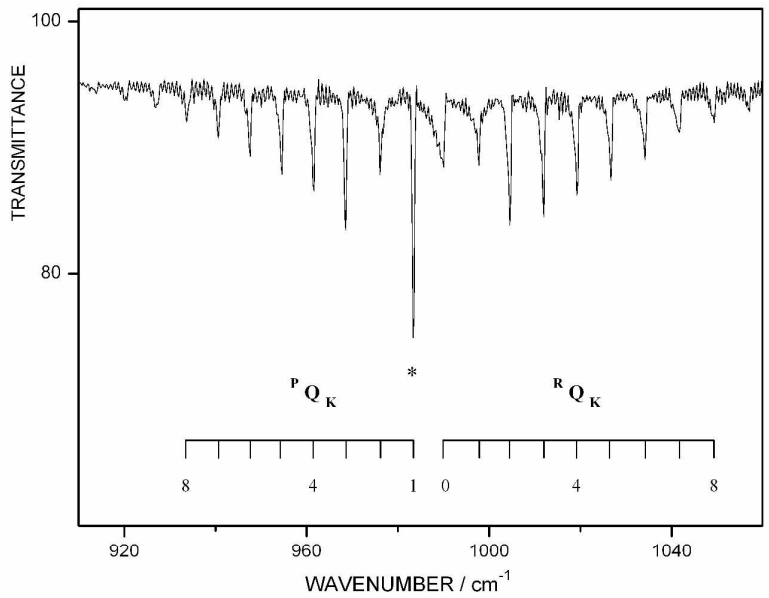

283x203mm (300 x 300 DPI)

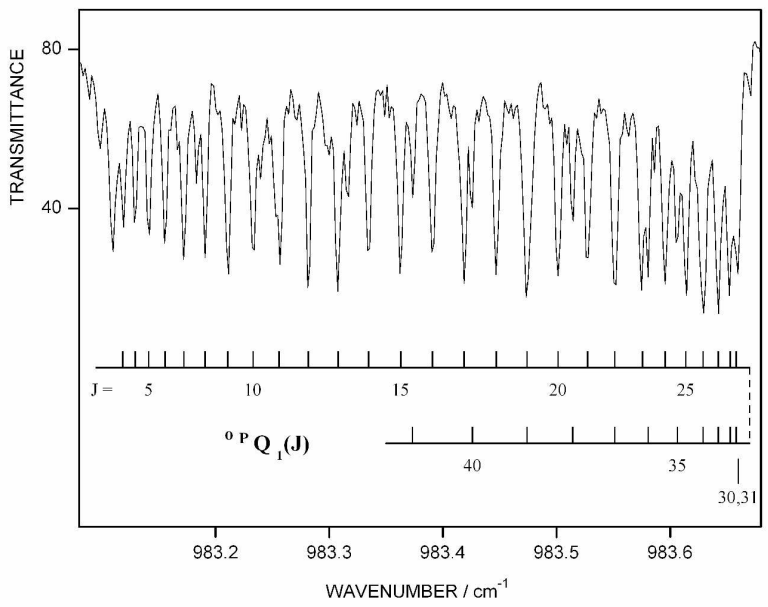

283x203mm (300 x 300 DPI)

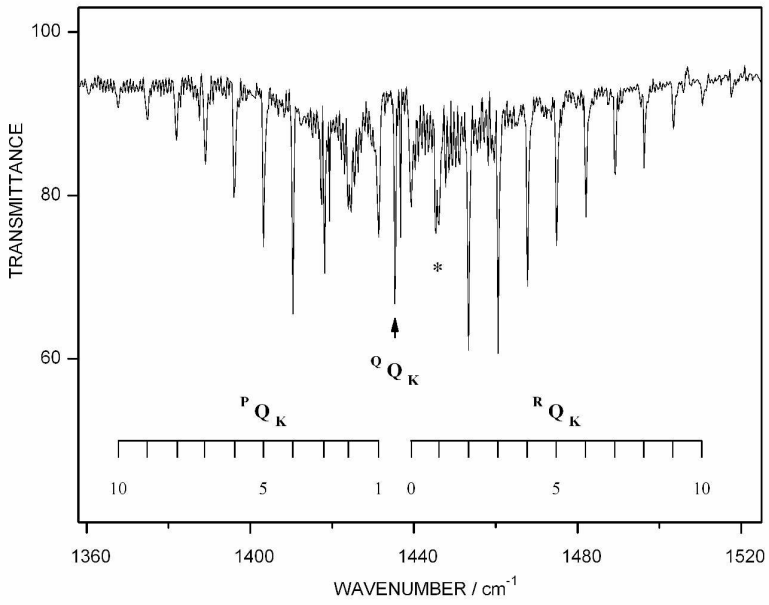

283x203mm (300 x 300 DPI)

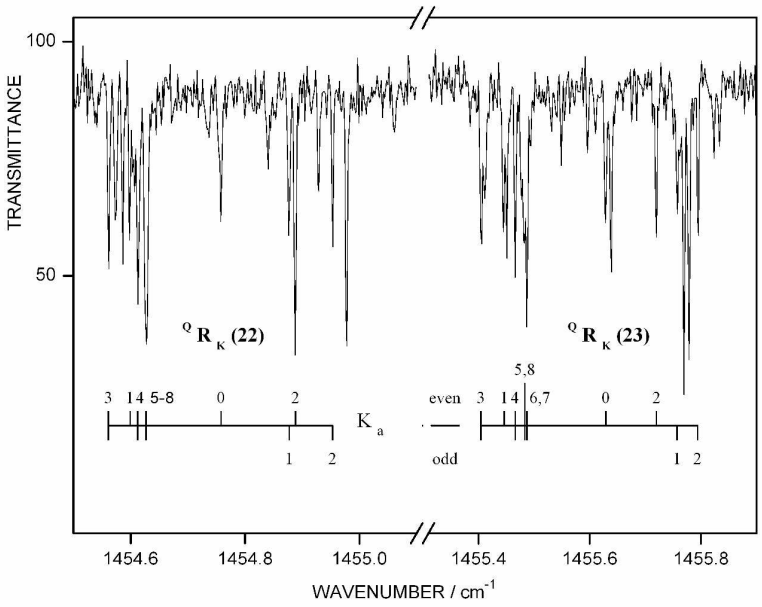

283x203mm (300 x 300 DPI)

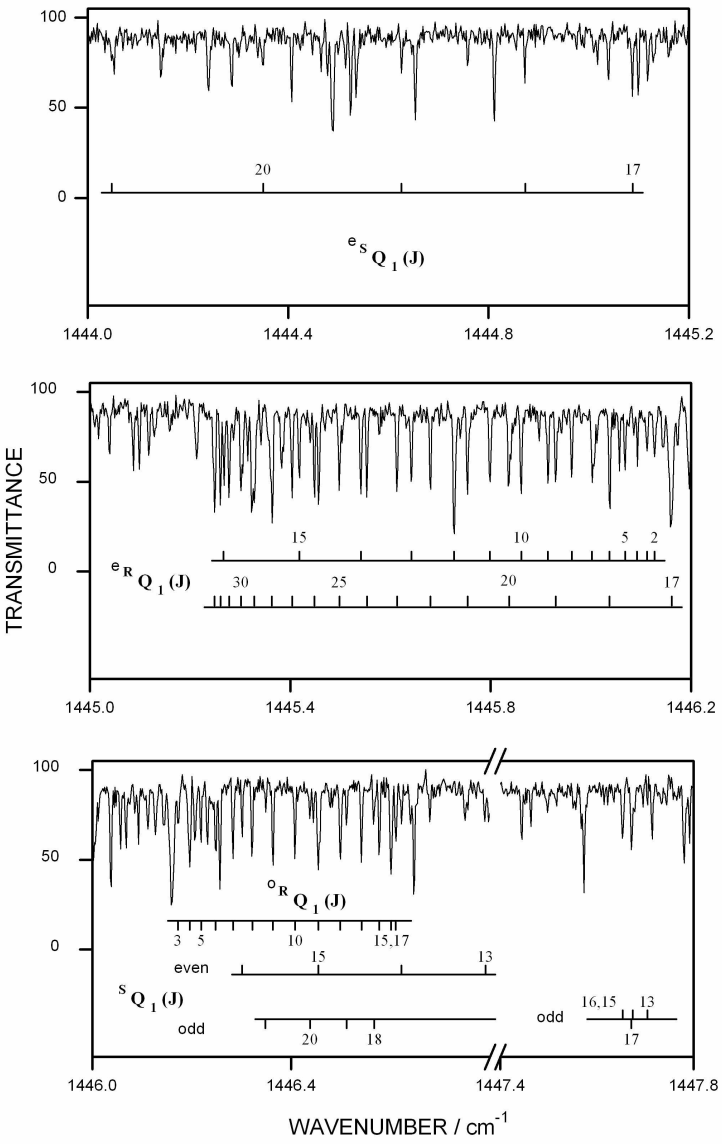

203x283mm (300 x 300 DPI)

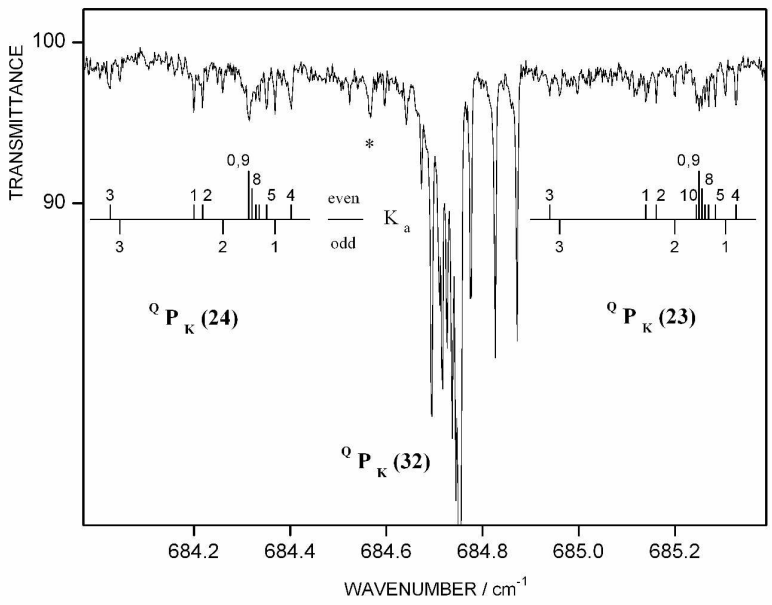

283x203mm (300 x 300 DPI)